Atmos. Chem. Phys. Discuss., 9, 5809–5852, 2009
www.atmos-chem-phys-discuss.net/9/5809/2009/

Atmospheric Chemistry and Physics Discussions

This discussion paper is/has been under review for the journal *Atmospheric Chemistry and Physics (ACP)*. Please refer to the corresponding final paper in *ACP* if available.

Distribution and sources of bioaccumulative air pollutants at Mezquital Valley, Mexico, as reflected by the atmospheric plant *Tillandsia recurvata* L.

A. Zambrano García[1], C. Medina Coyotzin[1], A. Rojas Amaro[1], D. López Veneroni[1], L. Chang Martínez[2], and G. Sosa Iglesias[1]

[1]Dirección Ejecutiva de Investigación y Posgrado, Instituto Mexicano del Petróleo, México D.F., Mexico
[2]Universidad Michoacana de San Nicolás de los Hidalgo, Morelia, Mexico

Received: 21 January 2009 – Accepted: 28 January 2009 – Published: 4 March 2009

Correspondence to: A. Zambrano García (azambran@imp.mx)

Published by Copernicus Publications on behalf of the European Geosciences Union.

Abstract

Mezquital Valley (MV), a Mexican wastewater-based agricultural and industrial region, is a "hot spot" of regulated air pollutants emissions, but the concurrent unregulated ones, like hazardous metals and polycyclic aromatic hydrocarbons (PAH), remain undocumented. A biomonitoring survey with the epiphytic *Tillandsia recurvata* was conducted there to detect spatial patterns and potential sources of 20 airborne elements and 15 PAH. The natural δ^{13}C and δ^{15}N ratios of this plant helped in source identification. The regional mean concentrations of most elements was two (Cr) to over 40 times (Ni, Pb, V) higher than reported for *Tillandsia* in other countries. Eleven elements, pyrene and chrysene had 18–214% higher mean concentration at the industrial south than at the agricultural north of MV. The total quantified PAH (mean, 572 ng g^{-1}; range, 142.6–2568) were composed by medium (65%, phenanthrene to chrysene), low (28%, naphthalene to fluorene) and high molecular weight compounds (7%, Benzo(*b*)fluoranthene to indeno(1,2,3-*cd*)pyrene). The δ^{13}C (mean, −14.6‰; range, −15.7 to −13.7‰) was lower (<−15‰) near the major petroleum combustion sources. The δ^{15}N (mean, −3.0‰; range, −9.9 to 3.3‰) varied from positive at agriculture/industrial areas to negative at rural sites. Factor analysis provided a five-factor solution for 74% of the data variance: (1) crustal rocks, 39.5% (Al, Ba, Cu, Fe, Sr, Ti); (2) soils, 11.3%, contrasting contributions from natural (Mg, Mn, Zn) and saline agriculture soils (Na); (3) cement production and fossil fuel combustion, 9.8% (Ca, Ni, V, chrysene, pyrene); (4) probable agricultural biomass burning, 8.1% (K and benzo(*g*,*h*,*i*)perylene), and (5) agriculture with wastewater, 5.2% (δ^{15}N and P). These results indicated high deposition of bioaccumulative air pollutants at MV, especially at the industrial area. Since *T. recurvata* reflected the regional differences in exposition, it is recommended as a biomonitor for comparisons within and among countries where it is distributed: southern USA to Argentina.

ACPD

9, 5809–5852, 2009

1 Introduction

Monitoring airborne metals, polycyclic aromatic hydrocarbons (PAH) and other bioaccumulative compounds with living organisms (biomonitoring) is a technique in use and refinement since at least the 1960's. It is a multipurpose environmental tool for exploring pollutant occurrence and dispersion trends at different geographical/time scales, to identify emission sources, estimate atmospheric deposition and relate biological/ecological changes to air pollution (Aboal et al., 2006; Conti and Cecchetti, 2001; Pirintsos and Lopi, 2008; Segala et al., 2008; Wolterbeek, 2002). Since bioaccumulative air pollutants usually travel in particles, biomonitoring is done preferentially with organisms that rely on the atmosphere as primary source of moisture and nutrients, such as lichens, mosses and some vascular plants. This dependence is indicated by positive correlations between the concentration of pollutants in the biomonitor tissues and the amount of atmospheric deposition (Sloff, 1995; St. Clair et al., 2002; Wolterbeek, 2002).

We report results from a biomonitoring survey of airborne metals and PAH at Mezquital Valley (MV) conducted in the context of the MILAGRO 2006 field campaign in Mexico. This region is environmentally better known by severe soil and water pollution problems caused by over 100 years of agricultural irrigation with untreated sewage water from Mexico City (Cifuentes et al., 1994; Down et al., 1999; Friedel et al., 2000; Siebe, 1994; Vázquez-Alarcón et al., 2001). Mezquital Valley is also a major Mexican "hot spot" in emissions of SO_2, particulate matter and other regulated pollutants by the Tula-Tepeji-Vito industrial corridor located there (SEMARNAT-INE, 2006). Nevertheless, there is very little information on the expected concurrence of unregulated air toxics at MV, such as hazardous metals, PAH and other persistent organic pollutants.

This survey explored MV for spatial deposition trends and potential sources of 20 trace and major elements and 15 hazardous PAH using the "ball moss" (*Tillandsia recurvata* L.) as a natural receptor. This epiphytic *Bromeliaceae* is very common at the study region, where it mainly grows on mesquite trees (*Prosopis laevigata* (Willd) M.C.

ACPD
9, 5809–5852, 2009

Johnst.). Adult individuals are spherical, ca. 10–12 cm in diameter, easy to recognize in the field and collect by hand. They have a reduced stem and non-functional roots. Most of their biomass is formed by linear leaves profusely covered with absorptive trichomes. This latter morphological feature increases the ability of this plant to capture moisture and particles directly from the surrounding air, which justifies naming it as an "air" or "atmospheric" plant (Schmitt et al. 1989). *Tillandsia recurvata* has some physiological resistance to high levels of O_3 and SO_2 (Benzig et al., 1992), which may partially explain why is it so abundant at the polluted MV. This and other atmospheric *Tillandsia* species have been used as in situ air pollution biomonitors in some southern US States and Latin-American countries, where this genus is exclusively distributed (e.g., De Sousa et al., 2007; Husk et al., 2004; Pignata et al., 2002; Pyatt et al., 1999; Schrimpff, 1984; Smodiš et al., 2004; Wannaz et al., 2006a,b). Successful transplanting of *Tillandsia* from rural into urban areas for the same purpose has been reported by Brighina et al. (2002); Figuereido et al. (2007) and Malm et al. (1998).

In addition to metals and PAH, the natural $\delta^{13}C$ and $\delta^{15}N$ stable isotope ratios were determined in the *T. recurvata* samples as further information to identify air pollution sources. The use of these plant ratios for such purpose is based upon their dependence on the isotopic composition of the C and N sources used by plants (e.g., Bukata and Kyser, 2007; Liu et al., 2008; Skinner et al., 2006; Solga et al., 2006). The $\delta^{13}C$ is useful in detecting fossil fuel emission sources because of the sharp difference between the C isotopic signature of petroleum and other fuels ($\delta^{13}C$=−20 to −35‰, Goldstein and Shaw, 2003) and that of natural unpolluted air ($\delta^{13}C$=−8‰). The ^{13}C-depleted gaseous and particulate emissions from petroleum combustion dilute this isotope in the air, causing a negative shift of the $\delta^{13}C$. Plants exposed to such polluted air incorporate C compounds impoverished in ^{13}C, like CO_2 for photosynthesis, and eventually manifest this in more negative $\delta^{13}C$ values (Lichtfouse et al., 2003; Norra et al., 2005). In contrast, the plant $\delta^{15}N$ changes cannot be as directly interpreted because of the many isotopic fractionation processes occurring within and between the N sources and the plant receptors. The natural $\delta^{15}N$ of land plants roughly ranges

from −7 to +9‰ (Kelly et al., 2005), but a plant δ^{15}N can be changed by the isotopic composition of its N sources and the ability of each plant species to discriminate against ^{15}N. In general, for plants obtaining this nutrient from atmospheric sources, if the emissions into the air are dominated by N compounds with more negative or less positive δ^{15}N than theirs, this ratio decreases. Such N compounds are usually reduced species (NH_y) abundant at, but not exclusive to, agriculture/farming areas. Contrarily, this ratio increases in plants predominantly exposed to N species with more positive or less negative δ^{15}N than theirs, mainly oxidized N species (NO_x) more common to urban/industrial areas because of the heavier use of fossil fuels (Jung et al., 1997; Skinner et al., 2006; Solga et al., 2005). Since agriculture and industry coexist at MV, we expected the *T. recurvata* δ^{13}C and δ^{15}N to reflect these land uses.

A data matrix with 50 MV sites and 38 chemical variables was reduced by standard univariate statistical techniques. Exploratory factor analysis (FA) of selected variables and mapping allowed us to detect the major regional emission sources. As far as we know, this is the first report on the bioaccumulative air pollution of MV using biomonitoring techniques.

2 Materials and methods

2.1 Study area

Mezquital Valley is located in Hidalgo State, Mexico, ca. 60 km NW of Mexico City (Fig. 1). It is a semiarid region (ca. 2429 km^2) with about 500 thousand inhabitants distributed in medium-size towns (e.g., Tula and Tepeji del Río) and many small villages. The mean annual temperature and precipitation range from 16.5°C and 432 mm at the north portion of the valley, which is mainly dedicated to agriculture, to 17.2°C and 647 mm at the industrialized south. The mean elevation at the agriculture flatlands is 2000 m above mean sea level, and up to 2400 m in the surrounding mountains. The original valley's vegetation was a xerophytic shrubland with "mesquite" tree

as dominant element. This vegetation disappeared at the agricultural areas and is now restricted to the foothills and highlands. Over 90 000 ha of MV are currently dedicated to agriculture with raw sewage water from Mexico City. This is the major cause of chemical and biological contamination of the regional soils (Siebe and Cifuentes, 1995). The Tepeji-Tula-Atitalaquia industrial corridor has about 140 industries, including a petroleum refinery (325 thousand barrels/day); a 1500 MW electricity power plant fueled with residual fuel oil and, secondarily, with natural gas, and over 20 small and large cement plants. That electricity plant is the largest emitter of air toxics among similar Mexican facilities (CEPAL-SEMARNAT, 2004). The regional cement production relies on raw limestone material obtained nearby by dusty open-sky mining operations. Cement is processed using residual fuel oil, petroleum coke and other materials, like used tiers and industrial wastes. Other MV industries include non-ferrous metal manufacturing, textile, chemical, processed food, and disposal, recycling or incineration of waste materials. Cabrera et al. (2003) estimated the MV emissions of total suspended particles (TSP) from industrial and mobile sources in 21 538 ton year^{-1}. This is a rather large amount, representing ca. 80% of the same emissions at the much larger and higher populated Mexico City (27 308 ton/year, SMA 2006). The contribution from natural and agricultural sources to the MV air pollution is still unknown. Two major regional natural/crustal sources of particulate material are the Cretaceous limestone (El Doctor Formation) that covers about 60% of MV, and mainly exposed at the E-SE sector (Silva-Mora, 1997), and Lower Tertiary igneous rocks, roughly located at the valley's west half.

2.2 Sampling and sample preparation

Tillandsia recurvata was sampled at 50 sites throughout MV in the late spring and early summer, 2006 (Fig. 1). Most sites were at mountain foothills where mesquite trees, from which the biomonitor was obtained, are more common. In a few sites lacking this tree, sampling was done on alternative trees and cacti. The mean elevation of the sampling sites was 2200 m (min, 1879 m; max, 2435 m). Three composite samples per

site were collected from tree branches at ≥1 m from the ground, each composed by six to eight "ball moss" individuals from different trees. Cross contamination between samples was avoided by wearing new dust-free latex gloves per sample. Samples were taken to the laboratory in air-dried condition in brown paper bags, and stored at ambient temperature until processing (late September/October, 2006). Prior chemical analyses, plant dead parts and extraneous materials like insects, feathers and spider webs were removed manually. Since *T. recurvata* is perennial, potential age-related variability in pollutant bioaccumulation was minimized by analyzing only the newest 3–4 pairs of leaves per shoot, representing probably one to two years of environmental exposition. The clean samples were subdivided into three portions for metal, PAH and isotopic analyses, and stored in polyethylene bags at −40°C until analyses.

2.2.1 Metals

The glass and Teflon material for sample digestion was cleaned by immersion in 10% HNO_3 (24 h) followed by profuse rinsing with deionized water. The plant samples were oven-dried to constant weight (70°C, three days) and ground to fine powder with agate mortar and pestle. A fraction of powder (0.15–0.2 g per sample) was digested with 6.0 ml HNO_3 (65%, Merck), 4.0 ml HCl (38%, JT Baker, Ultrex II), and 0.2 ml HF (48%, JT Baker, Ultrex II) in a microwave oven (Anton Paar, Multiwave 3000) using the "pine needles" program: phase I (power, 1400 W; ramp, 10 min; hold, 10 min; fan 1), phase 2 (power, 0 W; hold, 30 min; fan, 2). Digestion temperature: 180°C. The digests were filtered with Whatman 4 paper and brought to 25 ml with deionized water.

The elements were determined by inductively coupled plasma/optical emission spectrometry (ICP-OES, Perkin–Elmer, Optima 3200 DV) following the USEPA 6010C method (EPA, 2000). The sample injection flow was 1.0 ml min^{-1}. Calibration curves were prepared with diluted element standard solutions (High Purity). QC repeatability was checked up by injecting element mixtures (Ultra Scientific) every 10–15 samples. The percent recovery of seven certified elements in seven equally processed samples of the NIST 1575a standard reference material (trace elements in pine needles) was

(mean ± coefficient of variation): Al (102.2±2.0), Ca (113.5±10.1), Fe (117.3±7.5), Mg (84.8±13.9), P (96.5±2.0), Zn (83.0±5.1). The recovery of Ba was low (35.8±6.4%), but was very good for In (103.7±2.9%), which was added as surrogate from a 5.0 ppm standard solution.

2.2.2 PAH

The samples were organically extracted in microwave oven and analyzed by high performance liquid chromatography (HPLC) for the 15 PAH listed in Table 1. All glassware and Teflon materials for sample preparation were cleaned with liquid detergent (Liqui Nox), running water and consecutive rinsing with bidistilled water, acetone and dichloromethane (DCM). Samples (5 to 8 g, air-dry weight) were ground with ceramic mortar and pestle under liquid nitrogen. A fraction of powder (0.25–0.5 g) was oven-dried (90°C, 24 h) for dry weight determination and about 2.0 g were extracted in 10-sample batches with 30 ml DCM in microwave oven (CEM, model MarsX). The oven was programmed as USEPA 3546 method: potency, 1200 W; pressure, 100 psi; temperature, 115°C; time, 15 min; total extraction time, 30 min; cooling, 2 h. Each extraction batch included one pure DCM blank and one positive laboratory control sample (LCS). As a surrogate for the vegetal matrix, the LCS were added 0.5 g of dehydrated and deactivated Cromosorb (60/80 mesh, Supelco, Inc; 400°C for 4 h) and 200 µl of standard mixture containing 5 µg/ml of each target PAH (Chemservice). The extracts were filtered through Millipore membrane and concentrated to 1.0 ml under a gentle stream of ultrapure nitrogen supplied with a nitroevaporator (8158, N EVAP111, Organomation Associates, Inc). The concentrates were cleaned up with glass chromatographic columns (40 cm length × 1.5 cm ID) filled with deactivated (400°C for 4 h) alumina-silica-gel (USEPA 3610B and 3630C). The columns were packed from bottom to top with 1.0 cm silanized glass fiber (Alltech) humidified with DCM, 10 g alumina (Baker, Inc.,), 3.0 g silica gel (60/200 mesh, Mallincroft) and 2.0 g anhydrous sodium sulfate (JT Baker) dissolved in DCM. For final PAH separation, extra DCM (30 ml) was added to the columns. Eluates were captured in glass vials, concentrated to 1.0 ml

under ultrapure nitrogen, changed into acetonitrile (4.0 ml, Burdick & Jackson), filtered with 0.2 µm acrodiscs (Pall Gelman Laboratory), reconcentrated to 500 µl with ultrapure nitrogen and stored at −40°C in amber glass vials until analyses.

The extracts were analyzed with a liquid chromatograph (Agilent HP, 1100 series) equipped with Nucleosil column (Macherey-Nagel, 265 mm, 100-5 C18 PAH), an automatic sample injector, and DAD and fluorescence detectors. The analyses were done in 10-sample batches plus one blank and one positive control. Each batch had its own calibration curve with seven concentrations (0.0625 to 5.0 µg/ml) of stock acetonitrile solution containing 5 µg/ml of each target PAH. Samples were added 150 µl of 4,4′-difluorobifenil (Chemservice) solution in acetonitrile (4 µg/ml) as internal standard. Solvents A (methanol, 50%; acetonitrile, 25%; HPLC water, 25%) was injected from 0 to 3 min and gradually exchanged by solvent B (acetonitrile) from 3 to 21 min; only solvent B was injected from 21 to 35 min. Injection volume, 5 µl; flux, 0.3 ml/min; column temperature, 25°C; wavelength (FLD: 275–495 nm, Table 2; DAD: 230 nm); total analysis time per sample extract, 30 min. Method validation parameters: linearity (R^2<.98); accuracy and precision (RSD<3%); detection limit, (1.0 µg ml^{-1}); quantification limits, 0.01 to 0.03 µg ml^{-1}, depending on the compound (Table 1).

2.2.3 δ^{13}C and δ^{15}N

Air-dried samples (200–500 µg) were ground with cleaned ceramic mortar and pestle under liquid nitrogen, and dried at 80°C for 24 h. The δ^{13}C and δ^{15}N ratios were determined with a dual carbon and nitrogen analyzer coupled to a continuous flow isotope ratio mass spectrometer (Europa Scientific). Equipment precision was 0.1‰ for C and 0.2 ‰ for N. The isotopic composition is defined by:

$$\delta^{13}\mathrm{C} \quad \text{or} \quad \delta^{15}\mathrm{N}(‰) = (R_{\text{sample}}/R_{\text{standard}} - 1) \times 1000$$

where R is the sample or standard ratio of the heavy to the light isotope: ^{13}C/^{12}C and ^{15}N/^{14}N. The VPDB (Pee Dee Belemnite) and atmospheric nitrogen were used as standards to determine δ^{13}C and δ^{15}N, respectively (Mariotti, 1974; Coplen, 1995).

2.3 Statistics

The raw site-pollutant data base was regionally summarized by simple central tendency and dispersion statistics. The geographical distribution of pollutant was explored by mapping with a geostatistical gridding method for irregularly spaced data (Surfer, Ver. 7.05, Kriging method) and comparing concentrations between and among MV areas with *t*-tests or ANOVA, as appropriate. Potential emission sources were explored by factor analyses (FA) with principal component extraction and normalized varimax rotation (Statistica, Ver. 6.0). Since 50 sampling sites was a small number of cases, FA was used conservatively. Only 20 pollutants were included in FA to keep a 2.5 site to variable ratio. The standardized median site values were used for FA. Pollutants excluded from this analysis had one or more of the following problems: they were not detected or below quantification levels at ≥8 sampling sites (i.e., 16% of sites: Pb, Sb, B*a*A, B*b*F, B*k*F, B*a*P and I*cd*P); high skewness (>2) and/or kurtosis (>7); strong deviation from normality even after log transformation (Shapiro-Wilk test); no significant correlation with any other pollutant, because they tended to form factors with single pollutants (e.g., Cd and Cr), or contrarily, very high correlation (r>.9), which may lead to multicollinearity. All low and some medium molecular weight PAH, which predominantly disperse in the gas phase, were also excluded from FA (NAP, ACY, ACE, FLN, PHE, ANT and FLT). Finally, the pollutant selection for FA was aided by considering element signal to noise ratios (SNR), which relate the regional to the site variability, as defined by Wolterbeek et al. (1996), and the element enrichment factors (EF) calculated as

$$EF = (X_s/Al_s)/(X_r/Al_r)$$

where X_s and Al_s are the sample element and aluminum concentrations (ppm), respectively; X_r and Al_r are the element and aluminum concentrations (ppm) in the main crustal rocks of MV: limestone, according to Lozano and Bernal (2005), and igneous rocks, using averaged data from an internet data base by Surendra (2001).

ACPD
9, 5809–5852, 2009

3 Results and discussion

Mezquital Valley was biomonitored with *T. recurvata* to detect the regional dispersion trends and potential emission sources of airborne metals and PAH.

3.1 Metals

Table 2 summarizes the regional element concentrations in the biomonitor *T. recurvata*. Calcium was the most abundant element (regional mean, 1.3% on dry weight basis; min, 0.5%; max, 4.5%). This indicated high regional exposure to limestone dust at MV, which is exacerbated by the cement industry. Predominance of Ca in lichen biomonitors growing near a cement plant was recently reported by Branquinho et al. (2007). They considered this element as the best indicator for cement-dust. Other geochemically major elements followed Ca in abundance (%): K (0.76)>Al (0.42)>Na (0.34) > Mg (0.29)>Fe (0.17)>P (0.05)>Ti (0.02)>Mn (0.008).

The trace element constituted individually less than 0.005% of the *T. recurvata* dry biomass: V (0.0044)>Zn (0.0042)>Ba (0.0038)>Pb (0.0034)> Sr (0.0031)>Li (0.0018)>Ni (0.0016)>Cu (0.0007)>Cr (0.0006) >Sb (0.0005)>Mo (0.0004)>Cd (0.0002). The prevalence of V, an element typically abundant in crude oils (Bairwise, 1990), can be attributable to emissions from the major industrial users of petroleum fuels at MV. This will be detailed later.

At the gross level of data reduction in Table 2, the element concentrations in *T. recurvata* reflected the composition of the MV crustal rocks and agriculture soils (Fig. 2). According to this figure, there was a closer chemical similarity between the biomonitor and the igneous rocks (R^2=.86) than for soils (R^2=.78) and limestone (R^2=.64). Thus, a high proportion of the spatial element variability in the biomonitor could be expected to derive from these sources.

Most measured elements had higher mean concentrations than reported for other *Tillandsia* biomonitors in other US and Latin American areas. This is shown in Table 3 by the element concentration ratios between MV and other countries (MV:OT). This

ACPD
9, 5809–5852, 2009

ratio was ≥2 in 25 out of 44 cases in Table 3, which implies ≥100% higher bioaccumulation by the Mexican *Tillandsia* and, assuming similar interspecies ability to capture and retain airborne metals, at least equally higher atmospheric deposition at MV. Such difference was larger for anthropogenic elements like Ni, Pb and V, whose concentrations were, respectively, 79, 66 and up to 43 times as high as for *Tillandsia* biomonitors reported for Argentina (Wannaz et al., 2006a,b). The MV:OT ratio was <1.0; i.e., lower element concentration in *Tillandsia* at MV, in 11 cases (Table 3). Most of them involved Cu and Zn biomonitored within urban/industrial areas at São Paulo, Brazil (Figuereido et al., 2007), and Cali and Medellin, Colombia (Schrimpff, 1984). This is in part due to the fewer rural sites included in these later studies, since they are usually less exposed to anthropogenic emissions and tend to lower the mean concentrations calculated at the regional level.

3.2 PAH

Table 4 summarizes the regional concentration and variability of PAH in the biomonitor. The sum of quantified PAH per site ranged from 143 to 2568 ng g^{-1}, with regional mean and median equal to 572 and 439 ng g^{-1}, respectively, indicating a data distribution skewed to the right. Apart from PHE and CHR, which were lognormally distributed, the rest of PAH had neither normal nor lognormal distributions. The regional variability of PAH depended on the compound, ranging from 58% (ACY) to 165% (FLN). The medium molecular weight PAH (MMW: PHE, ANT, FLT, PYR, B*a*A and CHR) was the most abundant group, representing 64.5% of the total measured PAH. The low molecular weight PAH (LMW: NAP, ACY, ACE and FLN) constituted 28.1%, and the high molecular weight (HMW: B*b*F, B*k*F, B*a*P, B*ghi*P and I*cd*P) only 7.3%. The relatively low amount of the most hazardous PAH group (HMW) deserves further research to be explained. Hypothetically, it may be attributed to photodegradation enhanced by the high solar irradiation rates received in this tropical semiarid region and the scarce protection from it provided by the very open local vegetation.

The most frequent PAH were FLT, FLN, PHE and PYR, which were present at all

ACPD
9, 5809–5852, 2009

sampled sites, as well as CHR, NAP and B*ghi*P, which were missing only at one or two sites. Most HMW PAH had low to very low frequencies. For instance, B*a*P had quantifiable levels at only nine sites, and B*a*A, B*k*F and I*cd*P at the two sites closest to the petroleum refinery and the electrical power plant (Fig. 1). The most abundant compounds were FLT (24.2% of total quantified PAH, regional average), PHE (17.1%) and NAP (10.4%).

Table 5 compares the mean total PAH in *T. recurvata* at MV with other biomonitoring studies using *Tillandsia*. Such comparisons are, however, limited by the several factors affecting the total sum of PAH; e.g., the number and type of measured compounds, the biomonitor's ability to capture and retain them, and design aspects of the biomonitoring studies; e.g., number and type of sampling sites, length of exposure and sampling strategy (in situ vs. transplanted samples). No difference was clear between the total PAH at MV and one heavily polluted site at Mexico City measured by Wang et al., (2007) with pine needles, a morphologically and physiologically different receptor. The mean total PAH reported for *T. usneoides* from polluted sites in Río de Janeiro (De Sousa et al., 2007) doubled the mean value at MV. Nevertheless, the most polluted MV sites had similar or slightly different total PAH (1284–1748 ng g^{-1}) than the polluted sites at Rio de Janeiro, and no MV site had lower total PAH than unpolluted Brazilian sites (93 to 175 ng g^{-1}). Levels of total PAH at MV were 70 to 140% higher than recorded for two different *Tillandsia* species transplanted from Costa Rica into downtown Florence, Italy, for eight months (Brighina et al., 2002).

3.3 δ^{13}C and δ^{15}N

The δ^{13}C and δ^{15}N isotopic ratios of *T. recurvata* showed that this epiphyte is less discriminant against ^{13}C and more discriminant against ^{15}N than most terrestrial plants, and their spatial patterns at MV reflected the regional differences in C and N emissions from the main land uses.

The regional δ^{13}C ratio (mean, −14.6‰; min, −15.7‰; max, −13.7‰) was similar to known values for this species (−15.3 to −13.2‰, Martin, 1994) and within range for

Tillandsia with crassulacean acid metabolism (CAM; $\delta^{13}C > -20‰$, Crayn et al., 2004); i.e., plants which fix CO_2 predominantly at night as a water-saving adaption to arid environs (Pierce et al., 2002). This ratio was the most homogeneous of the measured variables. It varied only 2‰throughout MV (CV, 9.0%). Its less negative values occurred at the predominantly rural NW sector of the valley ($\delta^{13}C = -14.3‰ \pm 0.13$, mean ±standard error), being on average 0.6‰ higher than at the industrialized SE sector ($-14.9‰ \pm 0.12$; $p < .006$ from one-way ANOVA by sectors). This suggests that "background" regional $\delta^{13}C$ values for this plant may be similar to those at the NW sector (−14.3‰, on average).

The $\delta^{13}C$ decreased in *T. recurvata* from the rural periphery of MV ($\geq -14.5‰$) toward the core industrial area ($\leq -15‰$, Fig. 3a). This negative shift reflected the increased emissions of ^{13}C-depleted compounds from industrial fossil fuel combustion. This shift was expectable because crude petroleum and its combustion subproducts have more negative $\delta^{13}C$ values (−20 to −35‰, Goldstein and Shaw, 2003; Pichlmayer et al., 1998) than *T. recurvata*. This was confirmed by the regional positive correlation between the biomonitor's $\delta^{13}C$ and the Ni/V ratio ($r = .39$, $p = .01$), which was even closer ($r = .70$, $p = .001$) when considering only the sampling sites within a belt transect in the predominant wind direction (NE-SW, Fig. 4). These ratios had a parallel pattern along that transect, including a sharp decline at the sites located downwind of the main electric power plant and the refinery.

The spatial pattern of $\delta^{15}N$ reflected the emissions of this element from agriculture and industrial land uses at MV. Its regional mean was −3.0‰ (min, −9.9‰; max, 3.3‰), which represented 6 to 9.6‰ enrichment in ^{15}N with respect to other Mexican atmospheric *Tillandsia* from less polluted habitats ($\delta^{15}N = -9.0$ to $-12.6‰$, Hietz and Wanek, 2003; Hietz et al., 1999). The lowest, probably "background" $\delta^{15}N$ values of *T. recurvata* occurred at the rural SW corner of MV ($\approx -7.0‰$ on average). Interestingly, this *Tillandsia* discriminates more strongly against ^{15}N than most land plants, whose $\delta^{15}N$ range from −7 to +9‰ (Kelly et al., 2005). Another factor possibly behind this feature of atmospheric *Tillandsia* may be a symbiotic association with N-fixing bacteria.

ACPD
9, 5809–5852, 2009

This is documented to occur in Mexican *T. recurvata* (Puente and Bashan, 1994), but this needs experimental work to be clarified.

The δ^{15}N spatial pattern of *T. recurvata* at MV changed from positive (>3.0‰) to negative (<−6.0‰) along the predominant wind direction (NE-SW, Fig. 3b). The most positive or slightly negative values occurred near agriculture and industrial/urban areas, whereas the most negative were recorded at the farther W-SW rural sites. Similarly high to low δ^{15}N spatial contrasts have been documented for plants growing at other industrial/urban or agriculture areas and rural/remote locations (Gerdol et al., 2002; Jung et al., 1997; Pearson et al., 2000; Solga et al., 2005). Such contrasts are in general attributed to the higher N emission/deposition by human activities in the former areas. This explanation finds support from the positive correlations often observed between plant δ^{15}N and the total N deposition (e.g., Pardo et al., 2007; Skinner et al., 2006). There are two major, probably supplementary, hypotheses about what causes the higher plant δ^{15}N at urban/industrial areas: (a) increased exposure to some oxidized N species (NO_x) mainly from fossil fuel combustion, and b) fractionating losses of the lighter ^{14}N compounds from the plants by leaching or nitrification processes with subsequent concentration of ^{15}N in the remaining N pools (Jung, 1997). A spatial contrast between the δ^{15}N of mosses sampled near agriculture areas (less negative values) and rural environs (more negative values) was reported by Solga et al. (2005). They found this contrast related to the NH_4:NO_3^+ ratio in the bulk N deposition. This ratio was higher at agriculture areas; i.e., it was inversely proportional to the moss δ^{15}N. This implies that increasing the proportion of NO_3^+ and/or other compounds with high δ^{15}N in the bulk deposition, like N_2O (+6.7 to +7.0‰, Brenninkmeijer et al., 2003) shift positively this plant ratio.

The positive δ^{15}N values in the biomonitor near the MV agriculture areas may be related to the heavy use of untreated wastewater for irrigation. There are no δ^{15}N data for this water, but it is reasonable to assume high positive values, as reported elsewhere for wastewater (δ^{15}N=+10 to +22‰, several sources). Soils and plants exposed to such N enriched water tend to acquire its high δ^{15}N values (Cole et al., 2004; Wigand

ACPD
9, 5809–5852, 2009

et al., 2007). This is most likely the case at MV, where agriculture soils have a net positive N balance despite the substantial loss that may occur by volatilization of N compounds from the open wastewater channels and during irrigation (Siebe, 1998). Specifying which N compounds accounted for the δ^{15}N distribution at MV was beyond the reach of this survey; however, it can be hypothesized that gaseous and particulate emissions of compounds with high δ^{15}N (e.g., N_2O and NO_3, respectively) from those channels and soils are large enough to shift the naturally negative δ^{15}N of *T. recurvata* toward positive values. Recent, spatially limited measurements (5 ha) on the emissions of N_2O from MV agriculture soils show rates varying from 0.01–0.04 mg m^{-2} h^{-1} prior irrigation with wastewater to 3.4 mg m^{-2} h^{-1} after irrigation; i.e., similar to fluxes from fertilized arable soils (González-Méndez, et al. 2008). Other regional activities, like burning of agriculture debris, may also contribute to the high δ^{15}N values of this plant.

The plant δ^{15}N in the core industrial area (0 to +3‰) was similar to values at the agriculture sites. This could be due both to in situ N emissions from fossil fuel combustion sources (signaled with C, E and R in Fig. 3b) and wind-transported N from the main agriculture areas located immediately to the north of the industrial park.

3.4 Pollutant distribution and potential emission sources

Some insights on the element spatial dispersion at MV can be derived from their regional variability in the biomonitor (Table 2). The average coefficient of variation was 51% and ranged from 19% (Li) to 141% (Sb). The elements with lower variability (e.g, Li, 19%, and K, 25%) were in general more homogeneously distributed throughout the region than those more variable (e.g., V, 83%, Cr, 72%). The former elements are more likely to be emitted by widely distributed sources; e.g., soil or crustal rocks, whereas the latter ones may derive from localized emission sources.

In looking for spatial patterns of the studied pollutants, the median site concentrations at the industrialized south of MV were compared by straight *t* tests against those at the predominantly agricultural north. Eleven elements (Al, Ba, Ca, Fe, Li, Mo, Ni,

ACPD
9, 5809–5852, 2009

Sr, Ti, V and Zn), and CHR and PYR had 18 to 214% higher concentrations at the industrial area ($p<.05$, Table 6), and none was significantly more concentrated at the agricultural north. Such spatial difference is partially illustrated in Fig. 5. This figure plots the site normalized median concentration of Ca, CHR, PYR and V within a belt transect oriented along the predominant wind direction (NNE to SSW), including the main types of particle emitters in the region. At the industrial area (≥0 km in Fig. 5), those pollutants had site concentrations up to 5.2 (Ca), 4.2 (CHR), 4.8 (PYR) and 29 (V) times higher than at the farthest north, rural location (Mixquiahuala, 37 km, or −37 km in Fig. 5). At sites near or within the main north agriculture area (−2 to −30 km in Fig. 5), most elements and PAH had intermediate concentrations.

Figure 6 illustrates four selected distribution patterns of pollutants as mapped with the median site data. Vanadium (Fig. 6a) had a well-defined single concentration peak 3.7 km to the south of the major petroleum processing and combustion facilities. Its concentration dropped concentrically from there, but at faster rate toward the north than to south, indicating air transport in this direction. The V concentration slightly increased again southward (ca. 12 km from the main peak) probably due to further fossil fuel emissions from cement industries, which are heavy users of residual petroleum and other materials (petcoke, natural gas, vehicle tires and a variety of residual materials).

Chromium had also a single high concentration peak (>20 mg kg^{-1}; Fig. 6b) located at the north end of the valley; i.e., upwind from the industrial park. Two potential sources causing this Cr peak are nearby polluted agriculture soils and mining operations for limestone. At the rest of the sampling areas, the biomonitor had rather similar Cr levels (≈5 mg kg^{-1}).

Calcium had two high concentration spots coinciding with two major limestone areas, where mining for raw cement materials occurs, one at the NE and the other at the SE of the study region (Fig. 6c). In general, this element was more concentrated at the East half of MV were limestone rocks predominate. Its maximum site concentration occurred in the SSE sector, where the largest cement plants are located.

Figure 6d shows the distribution of total PAH in *T. recurvata*. The highest concen-

ACPD
9, 5809–5852, 2009

trations were recorded at the south of MV, mainly to the E-SW of the core industrial area, and the lowest concentrations at the mostly rural NW sector, upwind with respect to urban/industrial areas. The tree concentration peaks in Fig. 6d were determined by the most abundant MMW (FLT and PHE) and LMW (NAP) PAH, probably reflecting vehicular emissions from the closest urban settlements.

Prior to factor analysis, the element signal-to-noise ratio and enrichment factors (EF) were considered together with other criteria for variable selection (see Statistic section). The average SNR was 4.1 (min, 2.1, Cd; max, 7.3, Ca, Table 2), which was good in terms of signal information for a biomonitoring survey compared to values reported by Wolterbeek et al. (1996) for lichen, mosses and tree bark biomonitors (1.3 to 3.4).

Figure 7 shows the mean element EF relative to the Al concentrations in the regional rocks. Enrichment values close to 1.0 are in general indicative of crustal origin; higher EF values, subjectively ≥5, indicate enrichment by anthropogenic emissions. Potassium, Ni, P, V and Zn were more enriched in the biomonitor than expected from their average abundance in the MV igneous and limestone rocks. Therefore, those elements are likely to derive from industrial (Ni, V and Zn) and, tentatively, agricultural sources (K and P). Sodium, in contrast, was enriched only with respect to limestone; whereas Ca and Cu were enriched with respect to igneous rocks. The rest of elements in Fig. 5, Ba, Cr, Mg, Mn, Sr and Ti, probably originated from regional crustal/soil sources. The natural emission of some elements can be enhanced by activities like mining. This could be the Ca and Cr cases at MV since their highest concentrations in the biomonitor occurred at sites close to limestone mining areas.

Tables 7 and 8 show a factor analysis solution for the 50×20 (sites x pollutants) standardized data matrix. Five factors or potential sources with eigenvalues >1.0 accounted for 74% the data variance. Most of this variability (39.5%) was associated with F1, which was significantly loaded (factor loadings >0.6) by Al, Ba, Cu, Fe, Sr and Ti, and to some extent by Ca (factor loading=0.49, Table 8). Such elemental composition indicates crustal sources. Since the elements loading on this factor peaked in concentration at the agriculture/industrial frontier, they could derive from wind-carried soil

dust in N to S direction. This factor could be more related to soil formed mainly by igneous parental material because its main elements are much richer in these rocks than in limestone. According to regional geochemical data (Lozano and Bernal, 2005; Verma-Surendra, 2001), Al, Ba, Cu, Fe and Ti are, respectively, 106, 48, 3, 1, 201 and 340 times more concentrated in the igneous rocks than in limestone.

Factor 2 (F2) accounted for 11.3% of the variance. It was loaded by Mg, Mn and Zn and may be related to soil sources. Interestingly, and contrasting with these elements, Na loaded negatively on this factor. This factor may thus distinguish inputs from natural (Mg, Mn and Zn) and saline agriculture soils. Sodium is the main cation in the MV irrigation wastewater (Cervantes-Medel and Armienta, 2004; Jimenez and Chávez, 2004). Siebe (1998) attributed this to Na transport by the wastewater from saline areas near Mexico City. Consistently, the biomonitor had the highest Na concentrations (4000 to 5000 mg kg^{-1}) within or near the MV agriculture areas (Fig. 8).

Factor 3 (F3) accounted for 9.8% of the variance. This factor was significantly loaded by PYR, V, CRY, Ni, Ca and, to some extent, Zn. It is clearly an industrial factor with pollutants derived from fossil fuel combustion and cement production (Ca). The presence of Ca on this factor is explained by the regional spatial correlation between the main fixed fossil fuel combustion sources and the main cement plants in the S-SE of MV. The negative loading of $\delta^{13}C$ within this factor confirmed its association with petroleum combustion. This is illustrated in Fig. 4 by comparing the $\delta^{13}C$ variation with the Ni:V ratio, another reliable indicator of petroleum combustion emissions. Figure 9 shows how the elements with mainly crustal origin (Al, Ba, Cu Fe, Sr and Ti) and the industrial pollutants (Ca, CRY, Ni, PYR, V and Zn) separate between the F1 and F3.

Factor 4 (F4) had 8.1% of the variance associated with it. It was loaded by K and benzo(*g*,*h*,*i*)perylene, tentatively deriving from biomass burning, which may include agriculture debris in the flatlands and forest fires in the highlands at the W side of MV.

Factor 5 (F5) accounted only by 5.2% of the variance. It was loaded by the $\delta^{15}N$ isotopic ratio and P. This factor may reflect emissions from MV agriculture with wastewater, characterized by large amounts of N compounds, mainly NH_4 and NO_3, (Cervantes-

ACPD
9, 5809–5852, 2009

Medel and Armienta, 2004; Jimenez and Chávez, 2004) and P (Ortega-Larrocea et al., 2001). Phosphorus may also derive from the use of agricultural pesticides, which often contain this element.

Although FA does not extract pure factor/sources, it acceptably distinguished contributions from the most relevant generic sources of particulate matter into the MV air. The element variability appeared mainly associated with natural/soil sources and agriculture activities (F1+F2+F4+F5, 64% of the total variance explained), whereas the PAH, especially CHR and PYR, and the elements Ca, Ni, V and Zn characterized the industrial fossil fuel combustion emissions: electricity generation, petroleum refining and cement production. Increasing the number of sampling sites may have allowed us to account for contributions of specific emission sources to the load of atmospheric bioaccumulative pollutants in the study region.

4 Conclusions

This study produced previously unknown information on the regional levels, sources and dispersion of airborne metals and PAH at MV. The results allowed us the following conclusions. The site to site variability of most metals and PAHs in *T. recurvata* at MV reflected a differential long-term exposure to them. In general, most metals and some PAH had higher concentrations at this region than reported for similar biomonitors in other countries. The chemical correlation between the biomonitor and the regional rocks and the results from factor analysis and the spatial distribution indicated that natural sources had a higher relative importance than agricultural and industrial ones on the variability of the studied pollutants. *Tillandsia recurvata* was confirmed as a good biomonitor for bioaccumulation of air pollutants. In addition, its relatively high "background" $\delta^{13}C$ and low $\delta^{15}N$ compared to most plants make this epiphyte a sensitive monitor for C and N sources. It may be thus useful to use it as a common natural receptor in comparative studies within and among Latin American countries and the southern US states. This would minimize potential variability from using different species.

ACPD
9, 5809–5852, 2009

Acknowledgements. This study was funded by the Mexican Oil Company (PEMEX, project F.21393) and the Mexican Petroleum Institute (D.00391), and conducted under the MILAGRO 2006 Mexico field campaign. We thank I. Garcí a Torres and J. Rojas for assistance in the sample preparation process, and Dr. M. Morán Pineda, executive of the IMP Gas Spectroscopy and Environmental Studies Laboratory, for logistical support.

References

Aboal, J. R., Real, C., Fernández, J. A., and Carballeira, A.: Mapping the results of extensive surveys: the case of atmospheric biomonitoring and terrestrial mosses, Sci. Total Environ., 356, 256–274, 2006.

Benzig, D. H., Arditti, J., Nyman, L. P., Temple, P. J., and Adams, J. P.: Effects of ozone and sulfur dioxide on four bromeliads, Environ. Exp. Bot., 32(1), 25–29, 1992.

Bairwise, A. J. G.: Role of nickel and vanadium in petroleum classification, Energ. Fuels, 4, 647–652, 1990.

Branquinho, C., Gaio-Oliveira, G., Augusto, S., Pinho, P., Máguas, C., and Correia, O.: Biomonitoring spatial and temporal impact of atmospheric dust from a cement industry, Environ. Pollut., 151(2), 292–299, 2008.

Brenninkmeijer, C. A. M., Janssen, C., Kaiser, J., Röckmann, T., Rhee, T. S., and Assonov, S. S.: Isotope effects in the chemistry of atmospheric trace compounds, Chem. Rev., 103, 5125–5161, 2003.

Brighina, L., Papini, A., Mosti, S., Cornia, A., Bocchini, P., and Galleti, G.: The use of tropical bromeliads (*Tillandsia* spp.) for monitoring atmospheric pollution in the town of Florence, Italy, Rev. Biol. Trop., 50(2), 577–584, 2002.

Bukata, A. R. and Kyser, T. K.: Carbon and nitrogen isotope variations in tree-rings as records of perturbations in regional carbon and nitrogen cycles, Environ. Sci. Technol., 41, 1331–1338, 2007.

Cabrera Ruíz, R. B. E., Gordillo Martínez, A. J., and Cerón Beltrán, A.: Inventario de contaminación emitida a suelo, agua y aire en 14 municipios del Estado de Hidalgo, México, Revista Internacional de Contaminación Ambiental 19(4), 171–181, 2003.

CEPAL-SEMARNAT.: Evaluación de las externalidades ambientales de la generación ter-

moeléctrica en México. http://www.semarnat.gob.mx/informacionambiental/Publicacion/ext.pdf, 2004.
Cervantes-Medel, A. and Armienta, M. A.: Influence of faulting on groundwater quality in Valle del Mezquital, Mexico. Geofísica Internacional, 43(3), 477–493, 2004.
Cifuentes, E., Blumenthal, U., Ruíz Palacios, G., Bennett, S., and Peasey, A.: Epidemiological panorama for the agricultural use of wastewater: The Mezquital Valley, Mexico, Salud Pública México, 36, 3–9, 1994.
Cole, M. L., Valiela, I., Kroeger, K. D., Tomansky, G. L., Cebrian, J., Wigand, C., McKinney, R. A., Grady, S. P., and Carvalho da Silva, M. H.: Assessment of a δ^{15}N isotopic method to indicate anthropogenic eutrophication in aquatic ecosystems, J. Environ. Qual., 33, 124–132, 2004.
Conti, M. E. and Cecchetti, G.: Biological monitoring: lichens as bioindicators of air pollution assessment – a review, Environ. Pollut., 114, 471–492, 2001.
Coplen, T. B.: Discontinuance of SMOW and PDB, Nature, 375, p. 285, 1995.
Crayn, D. M., Winter, K., and Smith, J. A. C.: Multiple origins of crassulacean acid metabolism and the epiphytic habit in the Neotropical family *Bromeliacea*, PNAS, 101(10), 3703–3708, 2004.
De Sousa Pereira, M., Heitmann, D., Reifenhäuser, W., Ornellas Meire, R., Silva Santos, L., Torres, J. P. M., Malm, O., and Körner, W.: Persistent organic pollutants in atmospheric deposition and biomonitoring with *Tillandsia usneoides* (L.) in an industrialized area in Rio de Janeiro state, southeast Brazil – Part II: PCB and PAH, Chemosphere, 67, 1736–1745, 2007.
Downs, T. J., Cifuentes-García, E., and Buffet, I. M.: Risk screening for exposure to groundwater pollution in a wastewater irrigation district of the Mexico City region, Environ. Health Persp, 107(7), 553–561, 1999.
EPA.: Method 6010C. Inductively Coupled Plasma-Atomic Emission Spectrometry, Revision 3, 30 pp., 2000.
Figuereido, A. M., Nogueira, C. A., Saiki, M., Milian, F. M., and Domingos, N.: Assessment of atmospheric metallic pollution in the metropolitan region of São Paulo, Brazil, employing *Tillandsia usneoides* L. as biomonitor, Environ. Pollut., 145(1), 279–292, 2007.
Friedel, J. K., Langer, T., Siebe, C, and Stahr, K.: Effects of long-term waste water irrigation on soil organic matter, soil microbial biomass and its activities in central Mexico, Biol. Fertil. Soils, 31(5), 414–421, 2000.
Flores-Delgadillo, L., Hernández-Silva, G., Alcalá-Martínez, R., and Maples-Vermeersch, M.:

Total contents of cadmium, copper, manganese and zinc in agricultural soils irrigated with wastewater from Hidalgo, Mexico, Revista Internacional de Contaminación Ambiental, 8(1), 37–46, 1992.

Gerdol, R., Bragazza, L., Marchesini, R., Medici, A., Pedrini, P., Benedetti, S., Bovolenta, A., and Coppi, S.: Use of moss (*Tortula muralis* Hedw.) for monitoring organic and inorganic air pollution in urban and rural sites in Northern Italy, Atmos. Environ., 36, 4069–4075, 2002.

Goldstein, A. H. and Shaw, S. L.: Isotopes of volatile organic compounds: an emerging approach for studying atmospheric budgets and chemistry, Chem. Rev., 103, 5025–5048, 2003.

González-Méndez, B., Siebe, C., Fiedel, S., Hernández, J. M., and Ruíz-Suárez, L. G.: N_2O emissions from soil irrigated with untreated wastewater in central Mexico, J. Soil Sci. Plant Nutr., 8(3), p. 185, 2008.

Hernández-Silva, G., Flores-Delgadillo, L., Maples-Vermeersch, M., Solorio-Munguía, J. G., Alcalá-Martínez, J. R.: Riesgo de acumulación de Cd, Pb, Cr y Co en tres series de suelos del DR03, Estado de Hidalgo, México, Revista Mexicana de Ciencias Geológicas, II(1), 53–61, 1994.

Hietz, P., and Wanek, W.: Size-dependent variation of carbon and nitrogen isotope abundances in epiphytic bromeliads, Plant Biol., 5, 137–142, 2003.

Hietz, P., Wanek, W., and Popp, M.: Stable isotopic composition of carbon and nitrogen and nitrogen content in vascular epiphytes along an altitudinal transect, Plant, Cell and Environ., 22, 1435–1443, 1999.

Huerta, L., Contreras-Valadez, R., Palacios-Mayorga, S., Miranda, J., and Calva-Vasquez, G.: Total element composition of soils contaminated with wastewater irrigation by combining IBA techniques, Nucl. Instrum. Meth. Phys. Res. B, 189, 158–162, 2002.

Husk, G. J., Weishampel, J. F., and Schlesinger.: Mineral dynamics in Spanish moss, *Tillandsia usneoides* L. (*Bromeliacea*), from Central Florida, USA, Sci. Total Environ., 321, 165–172, 2004.

Hwang, H. M., Wade, T. L., and Sericano, J. L.: Concentrations and source characterization of polycyclic aromatic hydrocarbons in pine needles from Korea, Mexico, and United States, Atmos. Environ., 37, 2259–2267, 2003.

Jimenez, B. and Chávez, A.: Quality assessment of an aquifer recharged with wastewater for its potential use as drinking source: “El Mezquital Valley” case, Water Sci. Technol., 50(2), 269–276, 2004.

Jung, K., Gebauer, G., Gehre, M., Hoffmann, D., Weißflog, L., and Schürmann, G.: Anthropogenic impacts on natural nitrogen isotope variations in *Pinus sylvestris* stands in an industrially polluted area, Environ. Pollut., 97(1–2), 175–181, 1997.

Kelly, S. D., Stein, C., and Jickells, T. D.: Carbon and nitrogen isotopic analysis of atmospheric organic matter, Atmos. Environ., 39, 6007–6011, 2005.

Liu, X. Y., Xiao, H. Y., Liu, C. Q., Li, Y. Y., and Xiao, H. W.: Stable carbon and nitrogen isotopes of the moss *Haplocladium microphyllum* in an urban and a background area (SW China): the role of environmental conditions and atmospheric nitrogen deposition, Atmos. Environ., 42, 5413–5423, 2008.

Lozano, R. and Bernal, J. P.: Characterization of a new set of eight geochemical reference materials for XRF major and trace element analysis, Revista Mexicana de Ciencias Geológicas, 22(3), 329–344, 2005.

Lucho-Constantino, C. A., Álvarez-Suárez, M., Beltrán-Hernández, R. I., Prieto-García, F., and Poggi-Varaldo, H. M.: A multivariate analysis of the accumulation and fractionation of major and trace elements in agricultural soils in Hidalgo State, Mexico irrigated with raw wastewater, Environ. Int., 31(3), 313–323, 2005.

Malm, O., de Freitas Fonseca, M., Hissnauer Miguel, P., Rodríguez Bastos, W., and Neves Pinto, F.: Use of epiphyte plants as biomonitors to map atmospheric mercury in a gold trade center city. Amazon, Brazil, Sci. Total Environ., 213(1–3), 57–64, 1998.

Mariotti, A.: Natural N-15 abundance measurements and atmospheric nitrogen Standard calibration, Nature, 311, 685–687, 1974.

Martin, C. E.: Physiological ecology of the *Bromeliaceae*, Bot. Rev., 60(1), 1–82, 1994.

Norra, S., Handley, L. L., Berner, Z., and Stüben, D.: ^{13}C and ^{15}N natural abundances of urban soils and herbaceous vegetation in Karlsruhe, Germany, Eur. J. Soil Sci., 56(5), 607–620, 2005.

Ortega-Larrocea, M. P., Siebe, C., Bécard, G., Méndez, I., Webster, R.: Impact of a century of wastewater irrigation on the abundance of arbuscular mycorrhizal spores in the soil of the Mezquital Valley of Mexico, Appl. Soil Ecol., 16(2), 149–157, 2001.

Pardo, L. H., McNulty, S. G., Bogs, J. L., and Duke, S.: Regional patterns in foliar ^{15}N across a gradient of nitrogen deposition in the northeastern US, Environ. Pollut., 149, 293–302, 2007.

Pearson, J., Wells, D. M., Seller, K. J., Bennett, A., Soares, A., Woodall, J., and Ingrouille, M. J.: Traffic exposure increases natural $^{1}5N$ and heavy metal concentrations in mosses, New Phy-

tol., 147(2), 317–326, 2002.
Pichlmayer, F., Schöner, W., Seibert, P., Stichler, W., Wagenbach, D.: Stable isotope analysis for characterization of pollutants at high elevation alpine sites, Atmos. Environ., 32(23), 4075–4085, 1998.
Pierce, S., Winter, K., and Griffiths, H.: Carbon isotope ratio and the extent of daily CAM use by *Bromeliaceae*, New Phytol., 156, 75–83, 2002.
Pignata, M. L., Gudiño, G. L., Wannaz, E. D., Plá, R. R., González, C. M., Carreras, H. A., and Orellana, L.: Atmospheric quality and distribution of heavy metals in Argentina employing *Tillandsia capillaris* as a biomonitor, Environ. Pollut., 129, 59–68, 2002.
Pirintsos, S. A., and Loppi, S.: Biomonitoring atmospheric pollution: the challenge of times in environmental policy on air quality, Environ. Pollut., 151(2), 269–271, 2008.
Puente, M. E., and Bashan, Y.: The desert epiphyte *Tillandsia recurvata* harbours the nitrogen-fixing bacterium *Pseudomonas stutzeri*, Can. J. Bot., 72, 406–408, 1994.
Pyatt, F. B., Grattan, J. P., Lacy, D., Pyatt, A. J., and Seward, M. R. D.: Comparative effectiveness of *Tillandsia usneoides* L. and *Parmotrema praesorediosum* (Nyl.) Hale as bio-indicators of atmospheric pollution in Louisiana (USA), Water, Air, and Soil Pollut., 111, 317–326, 1999.
Schmitt, A. K., Martin, C. E., and Lüttge, U. E.: Gas exchange and water vapor uptake in the atmospheric bromeliad *Tillandsia recurvata* L, Botan. Acta, 102, 80–84, 1989.
Schrimpff, E.: Air pollution patters in two cities of Colombia according to trace substances contents of an epiphyte *Tillandsia recurvata*, Water Air Soil Pollut., 21(1–4), 279–316, 1984.
Segala, E. A., Baêsso, B. M., and Domingos, M.: Structural analysis of *Tillandsia usneoides* L. exposed to air pollutants in São Paulo city-Brazil, Water Air Soil Pollut., 189, 61–68, 2008.
SEMARNAT-INE.: Inventario Nacional de Emisiones de México, 1999, Secretaría del Medio Ambiente y Recursos Naturales/Instituto Nacional de Ecología, México, D. F., 409 pp., 2006.
Siebe, C.: Acumulación y disponibilidad de metales pesados en suelos regados con aguas residuales en el distrito de riego 03, Tula, Hidalgo, México, Revista Internacional de Contaminación Ambiental, 10(1), 15–21, 1994.
Siebe, C.: Nutrient inputs to soils and their uptake by alfalfa through long-term irrigation with untreated sewage effluent in Mexico, Soil Use Manage., 14, 119–122, 1998.
Siebe, C. and Cifuentes, E.: Environmental impact of wastewater irrigation in central Mexico: an overview, J. Environ. Health Res., 5, 161–173, 1995.
Silva-Mora, L.: Geología volcánica y carácter químico preliminar de las rocas de la regón Tula-

Polotitlán, Estados de Hidalgo, México y Querétaro, México, Revista Mexicana de Ciencias Geológicas, 14(1), 50–77, 1997.
Skinner, R. A., Ineson, P., Jones, H., Sleep, D., Leith, I. D., and Sheppard, L. J.: Heathland vegetation as a bio-monitor for nitrogen deposition and source attribution using δ^{15}N values, Atmos. Environ., 40, 498–507, 2006.
Sloof, J. E.: Lichens as quantitative biomonitors for atmospheric trace element deposition, using transplants, Atmos. Environ., 29(1), 11–20, 1995.
SMA.: Gestión Ambiental del Aire en el Distrito Federal: Avances y Propuestas, 2000–2006, Secretaría del Medio Ambiente, Gobierno del Distrito Federal, México, 2006.
Smodiš, B., Pignata, M. L., Saiki, M., Cortés, E., Bangfa, N., Markert, B., Nyarko, B., Arunachalam, J., Garty, J., Vutchkov, N., Wolterbeek, H. Th., Steinnes, E., Freitas, M. C., Lucaciu, A., and Frontasyeva, M.: Validation and application of plants as biomonitors of trace atmospheric pollution- a co-ordinated effort in 14 countries, J. Atmos. Chem., 49, 3–13, 2004.
Solga, A., Burkhardt, J., Zechmeister, H. G., and Frahm, J. P.: Nitrogen content, ^{15}N abundance and biomass of the two pleurocarpous mosses *Pleurozium schreberi* (Brid.) Mitt. and *Scleropodium purum* (Hedw.) Limpr. in relation to atmospheric nitrogen deposition, Environ. Pollut., 134, 465–473, 2005.
Solga, A., Eichert, T., and Frahm, J. P.: Historical alteration in the nitrogen concentration and ^{15}N natural abundance of mosses in Germany: indication for regionally varying changes in atmospheric nitrogen deposition within the last 140 years, Atmos. Environ., 40, 8044–8055, 2006.
St. Clair, S. B., St. Clair, L. L., Mangelson, N. F., and Weber, D. J.: Influence of growth form on the accumulation of airborne copper by lichens, Atmos. Environ., 36, 5637–5644, 2002.
Surendra, P. V.: Geochemical and Sr-Nd-Pb isotopic evidence for a combined assimilation and fraccional crystallisation process for volcanic rocks from the Huichapan caldera, Hidalgo, Mexico, Lithos, 56(2–3), 141–164, 2001.
Vázquez-Alarcón, A., Justin-Cajuste, L., Siebe-Grabach, C., Alcántar-González, G., and de la Isla de Bauer, M. L.: Cadmio, niquel y plomo en agua residual, suelo y cultivos en el Valle del Mezquital, Hidalgo, México, Agrociencia, 35, 267–274, 2001.
Wannaz, E. D. and Pignata, M. L.: Calibration of four species of *Tillandsia* as biomonitors, J. Atmos. Chem., 53(3), 185–209, 2006a.
Wannaz, D. E., Carreras, H. A., Pérez, C. A., and Pignata, M. L.: Assessment of metal accumulation in two species of *Tillandsia* in relation to atmospheric sources in Argentina, Sci. Total

Environ., 361, 267–278, 2006b.
Wigand, C., McKinney, R. A., Cole, M. L., Thursby, G. B., and Cummings, J.: Varying stable nitrogen isotope ratios of different coastal marsh plants and their relationships with wastewater nitrogen and land use in New England, USA, Environ. Monit. Assess., 131, 71–81, 2007.
Wolterbeek, H. T.: Biomonitoring of trace element air pollution: principles, possibilities and perspectives, Environ. Pollut., 120, 11–21, 2002.
Wolterbeek, H. Th., Bode, P., and Verburg, T. G.: Assessing the quality of biomonitoring via signal-to-noise ratio analysis, Sci. Total Environ. 180, 107–116, 1996.

Table 1. Target PAH and HPLC analytical parameters.

PAH	FLD λ_{ex}-λ^{a}_{em} (nm)	RT[b] (min)	QL[c] (µg ml^{-1})
Naphthalene, NAP	275–350	4.29	0.03
Acenaphthylene, ACY	275–350	4.95	0.03
Acenaphthene, ACE	275–350	6.75	0.01
Fluorene, FLN	275–350	7.30	0.01
Phenanthrene, PHE	275–350	8.59	0.01
Anthracene, ANT	275–450	10.45	0.01
Fluoranthene, FLT	275–450	11.94	0.01
Pyrene, PYR	275–410	13.14	0.03
Benzo(*a*)anthracene, B*a*A	275–410	17.29	0.03
Chrysene, CHR	275–410	18.47	0.01
Benzo(*b*)fluoranthene, B*b*F	275–410	21.32	0.01
Benzo(*k*)fluoranthene, B*b*F	275–410	23.02	0.03
Benzo(*a*)pyrene, B*a*P	275–410	24.28	0.03
Benzo(*g*,*h*,*i*)perylene, B*g*P	275–410	27.56	0.01
Indeno(*1,2,3-cd*)pyrene, I*cd*P	275–495	29.01	0.03

[a] Fluorescence detector excitation (ex) and emission (em) wave length;
[b] retention time;
[c] Quantification limit.

ACPD
9, 5809–5852, 2009

Table 2. Regional summary of elements in *T. recurvata* at Mezquital Valley (mg/kg).

Element	*N*	*n*	Mean	Median	Range	CV (%)	S/N	*p*(*r*)	*p*(log)
Al	150	50	4155	3969	290–11 900	41.1	4.5		>.05
Ba	150	50	38.1	33.2	8.9–131	51.0	4.1		
Ca	149	50	12 556	10 190	2883–46 780	55.2	7.3		>.05
Cd	150	50	2.2	1.9	0.9–6.5	42.7	2.1		>.05
Cr	139	49	6.1	4.5	0.8–40.4	96.3	6.1		
Cu	150	50	7.0	5.9	2.0–48.4	71.6	3.5		>.05
Fe	149	50	1579	1444	401–4368	41.1	3.5		
K	150	50	7568	7559	1398–16,380	33.3	2.5	>.05	
Li	150	50	18.1	17.0	6.0–34.0	24.8	3.2		>.05
Mg	150	50	2906	2815	868–6285	33.8	2.7		>.05
Mn	149	50	80.3	75.2	14.2–327.4	39.4	4.3		>.05
Mo	145	47	4.0	4.0	0.3–28.6	76.6	5.5		
Na	149	50	3236	3046	424–10,280	57.6	6.1	>.05	
Ni	123	50	15.9	14.0	1.6–44.2	60.4	4.5		>.05
P	150	50	501	486	163–1642	45.1	3.8		>.05
Pb	86	31	33.1	28.6	1.4–226	92.0	3.6		
Sb	25	9	4.0	2.9	0.2–25.4	124.3	3.6		
Sr	148	50	30.5	28.4	1.9–83.2	44.8	2.8		>.05
Ti	150	50	196	177	58.0–532	42.8	2.8		
V	150	50	43.4	29.7	6.5–220	86.8	5.5		>.05
Zn	150	50	41.9	36.4	3.7–192	57.0	4.0		

N, number of samples; *n*, number of sampling sites with quantifiable element amount; CV, coefficient of variation; S/N, mean signal to noise ratio; *p*(r) and *p*(log), probability associated to Shapiro-Wilks normality tests for raw and $\log_{10}$ transformed data, respectively; empty cells, non-normal distribution.

Table 3. Regional mean element concentration (mg kg^{-1}) in *T. recurvata* at Mezquital Valley (MV) and *Tillandsia* from other countries (OC). Values in parentheses are the MV:OC ratio.

Element	MV	Argentina[a]	Argentina[b]	Brazil[c]	Colombia[d]	Colombia[e]	US[f]
Al	4155			1112 (3.7)			
Ba	38.1			36.8 (1)			
Ca	12 556			3312 (3.8)			4160 (3.0)
Cd	2.2				0.4 (5.3)	0.82 (2.6)	
Cr	6.1			2.2 (2.8)			
Cu	7.0	0.9 (7.8)	0.9 (7.0)	19.3 (0.4)	52.7 (0.1)	30.5 (0.2)	7.1 (1.0)
Fe	1579	223 (7.1)	257 (6.1)	1144 (1.4)			575 (2.7)
K	7568			5890 (1.3)			2550 (3.0)
Mg	2906			2025 (1.4)			414 (7.0)
Mn	80.3	22.6 (3.6)	22.3 (3.6)	174 (0.5)			52.8 (1.5)
Na	3,236			1923 (1.7)			
Ni	15.9	0.2 (79.4)	0.2 (79.4)		11.9 (1.3)	52.8 (0.3)	
Pb	33.1	0.5 (66.2)	0.5 (66.2)		40.6 (0.8)	26.3 (1.3)	
Sb	4.0			0.5 (8.0)			
V	43.4	1.0 (43.4)	1.1 (39.5)	2.7 (16.1)			
Zn	41.9	4.0 (10.5)	3.8 (11.0)	111 (0.4)	119 (0.4)	379 (0.1)	73.5 (0.6)

[a] Wannaz et al. (2006a), *T. capillaris*;
[b] Wannaz et al. (2006b), *T. permutata*;
[c] Figuereido et al. (2007), *T. usneoides*, average value for the two-months transplanting period presenting the maximum concentration, excluding the control site,
[d,e] Schrimpff (1984), Cali and Medellín cities, respectively;
[f] Husk et al. (2004), *T. usneoides* in Florida, samples recollected in 1998. Empty cells: data not reported.

ACPD
9, 5809–5852, 2009

Table 4. Regional PAH concentrations (ng g^{-1}) in *T. recurvata* at Mezquital Valley, Mexico.

HAP	*N*	*n*	Mean	Median	Range	CV (%)
NAP	141	49	82.3	49.6	6.0–607	122.8
ACY	85	40	88.6	78.8	10.2–292	61.9
ACE	51	32	19.6	13.4	1.1–87.0	95.6
FLN	129	50	37.6	21.4	7.2–386	134.6
PHE	150	50	136	114	9.9–624	60.3
ANT	92	42	9.0	7.1	1.7–27.0	63.0
FLT	150	50	192	72.2	19.3–1674	164.9
PYR	148	50	25.9	22.1	0.03–158.	88.0
B*a*A	2	2	12.8	12.8	0.2–25.4	139.7
CHR	127	49	22.5	18.2	1.9–92.9	72.6
B*b*F	75	40	18.3	13.2	0.1–131	118.0
B*k*F	2	2	13.5	13.5	1.7–25.3	123.6
B*a*P	12	9	41.7	39.9	2.4–87.6	58.2
B*ghi*P	112	48	28.1	22.5	4.0–134	73.7
I*cd*P	2	2	67.0	67.0	22.2–112	94.4
LMW	150	50	164	128	12.4–738	81.2
MMW	150	50	376	261	74.1–2131	96.8
HMW	122	50	42.5	32.8	0.1–250	85.0
ΣHAPs	150	50	572	439	142.6–2568	76.7

N, number of samples; *n*, number of sampling sites with quantifiable PAH amount; CV, coefficient of variation.

Table 5. Mean PAH concentration (ng g^{-1}) in *T. recurvata* at Mezquital Valley (MV) and for *Tillandsia* in other countries (OC). Values in parentheses are the MV:OC ratio.

HAPs	MV	Mexico City[a]	Sao Paulo, Brazil[b]		Florence, Italy[c]	
			Polluted sites	Unpolluted sites	*T. caput-medusae*	*T. bulbosa*
NAP	82.3		70.7 (1.2)	11.4 (7.2)		
ACY	88.6	8.3 (10.7)	10.2 (8.7)	1.4 (63.3)	23.4 (3.8)	55.1 (1.6)
ACE	19.6	1.7 (11.5)	13.7 (1.4)	8.6 (2.3)	53.6 (0.4)	53.9 (0.4)
FLN	37.6		24.6 (1.5)	9.5 (4.0)	4.0 (9.4)	112.1 (0.3)
PHE	136	15.8 (8.6)	198.2 (0.7)	18.6 (7.3)		
ANT	9.0	2.39 (3.8)	23.3 (0.4)	1.5 (6.0)	6.9 (1.3)	14.0 (0.6)
FLT	192	66.9 (2.9)	211.5 (0.9)	20.1 (9.6)		
PYR	25.9	118 (0.2)	145.1 (0.2)	14.2 (1.8)		
B*a*A	12.8	11.6 (1.1)	41.9 (0.3)	3.9 (3.3)	24.5 (0.5)	10.8 (1.2)
CHR	22.5	49.8 (0.5)	119.4 (0.2)	18.3 (1.2)	34.9 (0.6)	18.5 (1.2)
B*b*+*k*F	31.8	47.2 (0.7)	111.6 (0.3)	15.9 (2.0)		
B*a*P	41.7	9.2 (4.5)	72.7 (0.6)	4.0 (10.4)	8.26 (5.0)	35.0 (1.2)
B*ghi*P	28.1	39.7 (0.7)	29.3 (1.0)	5.0 (5.6)	28.2 (1.0)	
I*dc*P	67.0	28.2 (2.4)	31.1 (2.2)	3.9 (17.2)	33.2 (2.0)	12.4 (5.4)
ΣPAH	572	563 (1.0)	1067 (0.5)	138 (4.1)	238 (2.4)	330 (1.7)

[a] Hwang et al. (2007): measurements in *Pinus maximartinezii* needles at one site exposed to vehicle/industrial emissions.
[b] After de Souza Pereira et al. (2007): average of summer and winter measurements at four and three polluted and unpolluted sites, respectively, with *T. usneoides*.
[c] Values after an eight-month transplantation period into an urban site (Brighigna et al. 2002).

Table 6. Mean element (mg kg^{-1}) and PAH (ng g^{-1}) concentration in *T. recurvata* at Mezquital Valley.

Pollutant	North Mean±S.D.	South Mean±S.D (p-level).	D*
Al	3724±918.7	4625±2003.8 (.05)	24.2
Ba	31.0±6.62	43.5±18.20 (.01)	40.3
Ca	9453±4073.5	15 577±7078.9 (.001)	64.8
Cd	2.1±0.83	2.1±0.55	
Cr	5.9±6.06	4.7±2.15	
Cu	6.1±1.95	6.7±2.87	
Fe	1283±278.0	1848±701.9 (.001)	44.0
K	7078±2058.2	7786±1477.9	
Li	17.0±3.23	18.7±3.83	
Mg	2647±692.7	3111±970.6 (.05)	17.5
Mn	77.3±17.99	79.4±23.66	
Mo	3.2±1.71	4.8±3.25 (.05)	50.0
Na	3215±1414.4	2815±1421.4	
Ni	11.2±4.95	20.8±10.25 (.001)	85.7
P	478±130.5	505±234.6	
Sr	26.8±7.23	34.8±14.30 (.05)	29.9
Ti	164±34.5	230±92.5 (.01)	40.2
V	21.0±7.01	65.9±38.89 (.001)	213.8
Zn	31.4±6.90	52.0±27.82 (.01)	65.6
NAP	55.5±39.22	107±144.0	
FLN	26.9±25.10	46.9±73.27	
PHE	113±54.6	144±68.6	
FTN	136±265.6	159±171.0	
PYR	16.1±8.63	28.8±11.89 (.001)	78.9
CRY	14.8±7.17	27.3±16.76 (.01)	84.5
BGP	25.5±12.00	28.0±15.64	

*D percent South–North mean difference.

Table 7. Factor analysis of air pollutants in *T. recurvata* at Mezquital Valley.

	Eigenvalue	% Total variance	Cumulative eigenvalue	Cumulative %
1	7.899262	39.49631	7.89926	39.49631
2	2.255762	11.27881	10.15502	50.77512
3	1.956216	9.78108	12.11124	60.55620
4	1.610575	8.05287	13.72181	68.60907
5	1.049229	5.24614	14.77104	73.85522

Table 8. Factor loadings from varimax normalized rotation.

	F1	F2	F3	F4	F5
Al	**0.782141**	–0.296500	0.300588	0.080445	0.221772
Ba	**0.868804**	0.264733	0.144711	–0.072414	0.169377
Ca	0.493273	0.043636	**0.620724**	0.048071	0.329839
Cu	**0.613585**	0.440932	0.090640	0.270310	0.054297
Fe	**0.857248**	0.076959	0.315934	0.136890	0.192677
K	0.312873	–0.024921	–0.016092	**0.711933**	0.041798
Mg	0.353162	**0.675140**	0.130263	0.240675	0.208002
Mn	0.246131	**0.699433**	–0.142963	0.179151	–0.184237
Na	0.215081	**–0.712513**	–0.082735	0.365809	0.055969
Ni	0.122855	–0.279533	**0.726916**	–0.035345	–0.258114
P	0.420550	0.272611	0.173187	0.076305	**0.673771**
Sr	**0.720837**	0.264039	0.248782	–0.149863	0.210754
Ti	**0.891629**	0.072679	0.249946	0.115976	0.136683
V	0.327818	0.191190	**0.788638**	–0.015995	0.286278
Zn	0.243497	**0.656687**	0.567036	0.078629	0.192644
PYR	0.168647	0.048174	**0.809639**	0.121412	0.029343
CRY	0.232388	0.238241	**0.782127**	0.045808	0.336234
B*g*P	–0.199006	0.134764	0.139753	**0.724478**	–0.154185
δ^{13}C	–0.078791	–0.011390	–0.186589	–0.006616	**–0.733421**
δ^{15}N	0.260474	–0.193059	–0.045800	–0.199474	**0.688301**
Expl. Var	4.920120	2.623449	3.599062	1.467477	2.160934
Prp. Totl	0.246006	0.131172	0.179953	0.073374	0.108047

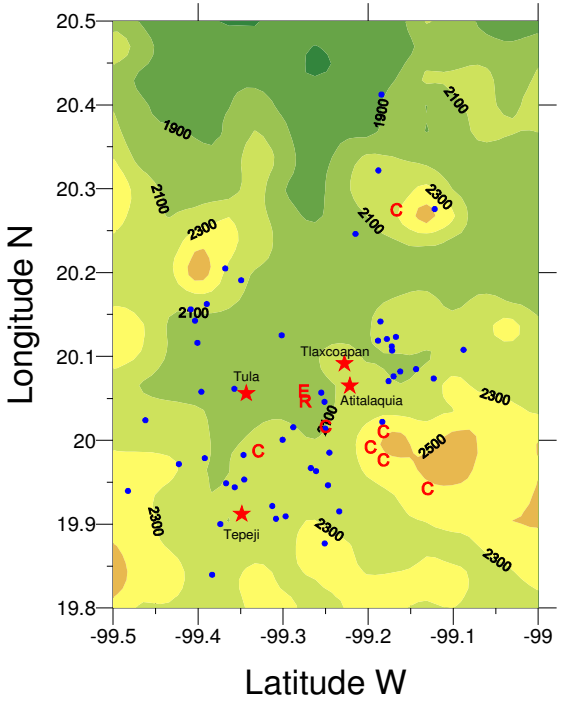

Fig. 1. Mezquital Valley study area. Symbols: dots, sampling sites; stars, main urban settlements; E, electricity power plant; R, petroleum refinery; C, cement plants. The isoline numbers indicate topographic elevation (m).

ACPD
9, 5809–5852, 2009

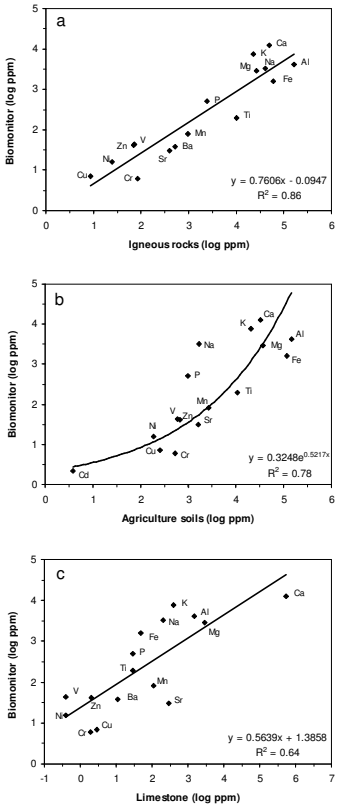

Fig. 2. Elemental concentrations in *T. recurvata* and crustal/soil sources at Mezquital Valley (log_{10} transformed mean values). Geochemical data: igneous rocks, mean values calculated from Verma-Surendra (2001); agricultural soils, median values among Flores-Delgadillo et al., (1992); Hernández-Silva et al., (1994); Huerta et al., (2002); Lucho-Constantino et al., (2005) and Siebe (1994); limestone (Lozano and Bernal 2005).

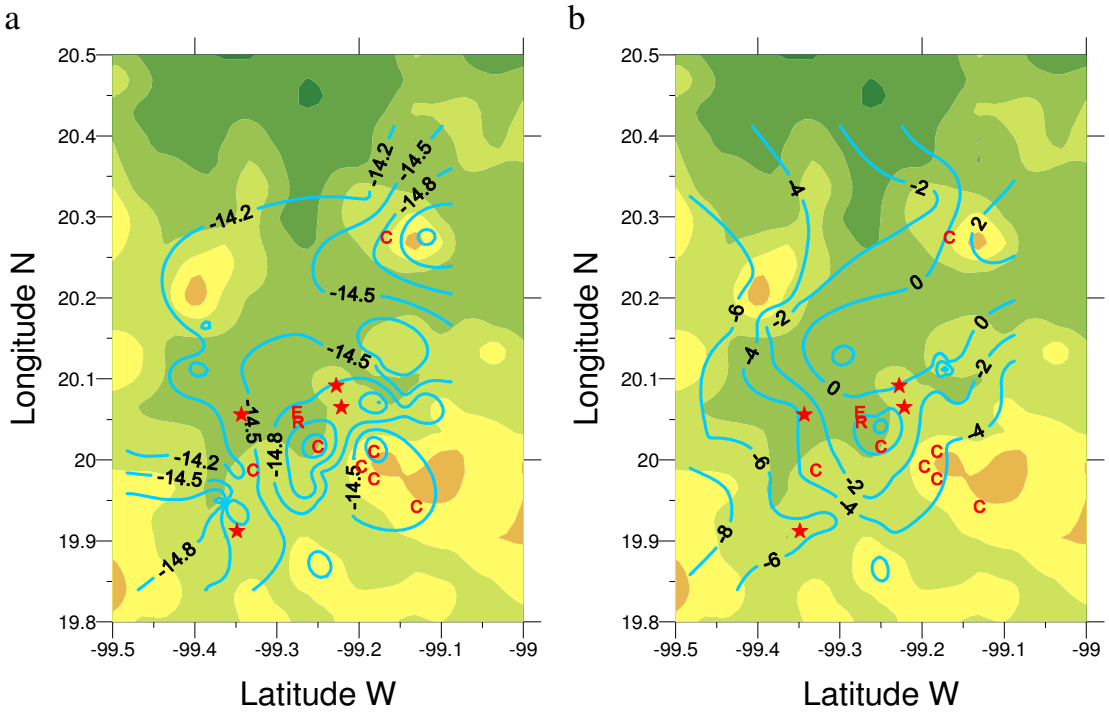

Fig. 3. Spatial distribution of the natural *T. recurvata* δ^{13}C **(a)** and δ^{15}N **(b)** isotopic ratios at Mezquital Valley.

ACPD
9, 5809–5852, 2009

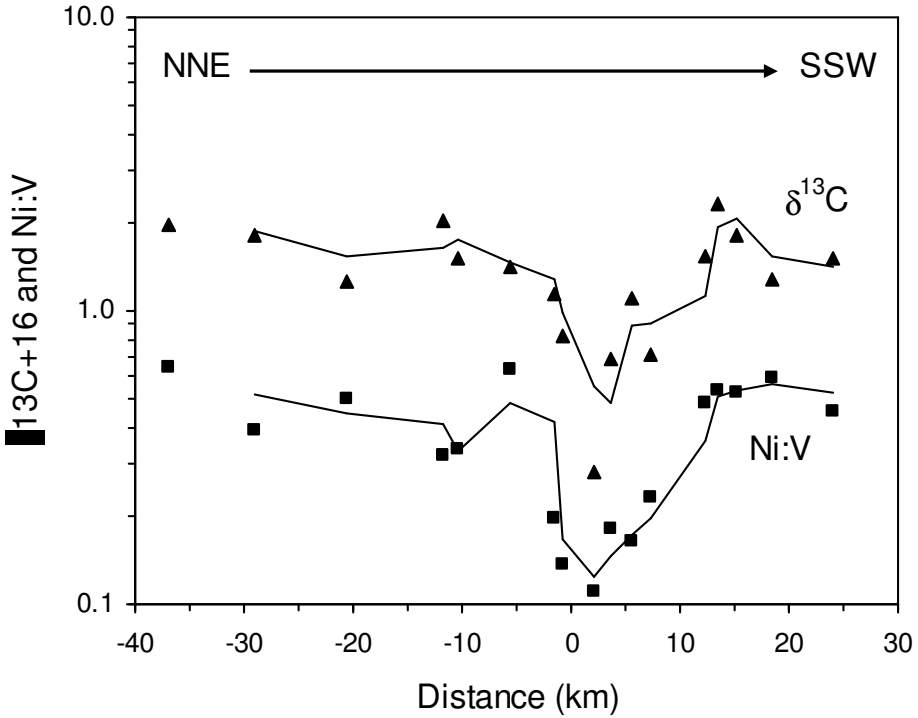

Fig. 4. Median δ^{13}C (triangles) and Ni:V ratios (squares) in *T. recurvata* at sites along a transect oriented with the predominant wind direction at Mezquital Valley (arrow). The main petroleum combustion sources are located at km 0. The δ^{13}C values were added 16 to allow the logarithmic transformation of the *y*-axis. The fitting lines are two-period running means.

ACPD
9, 5809–5852, 2009

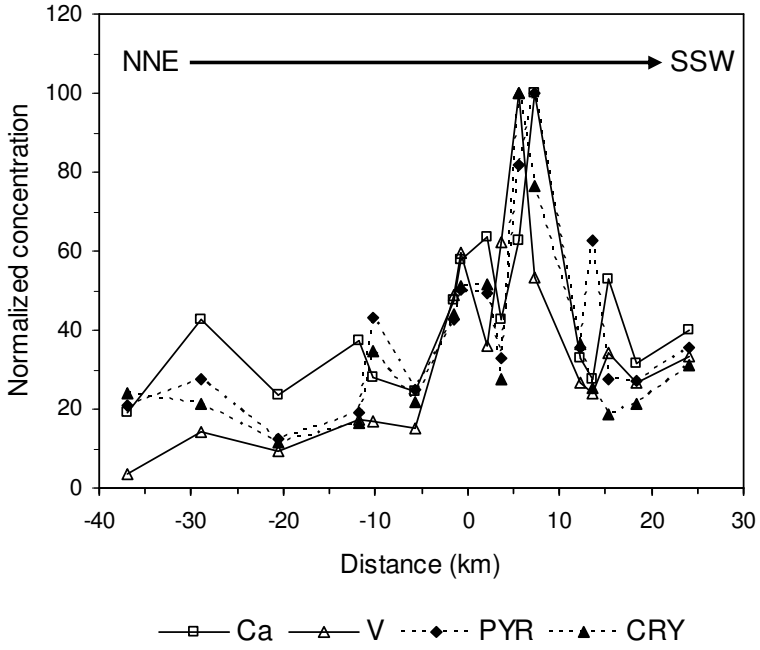

Fig. 5. Normalized median site concentration of two metals and two PAH in *T. recurvata* along a NNE-SSW transect at Mezquital Valley. The 100 value represents the maximum site concentration: Ca, 32 600 mg kg^{-1}; CRY, 82.1 ng g^{-1}; PYR, 65.9 ng g^{-1}; V, 197.2 mg kg^{-1}. The border between the main agricultural and industrial areas is roughly located at km 0.

ACPD
9, 5809–5852, 2009

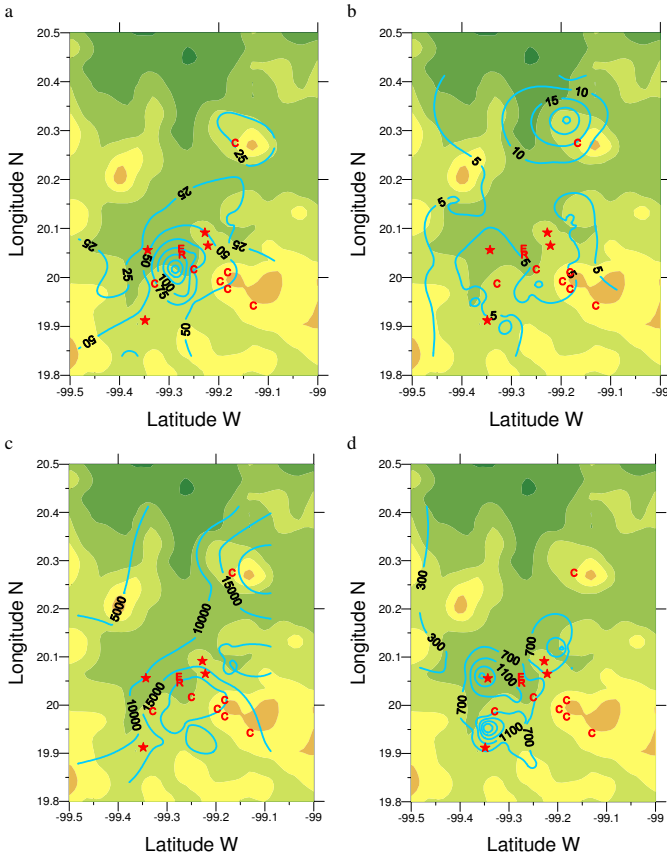

Fig. 6. Spatial distribution of V **(a)**, Cr **(b)**, Ca **(c)** and total PAH **(d)** in *T. recurvata* at Mezquital Valley.

ACPD
9, 5809–5852, 2009

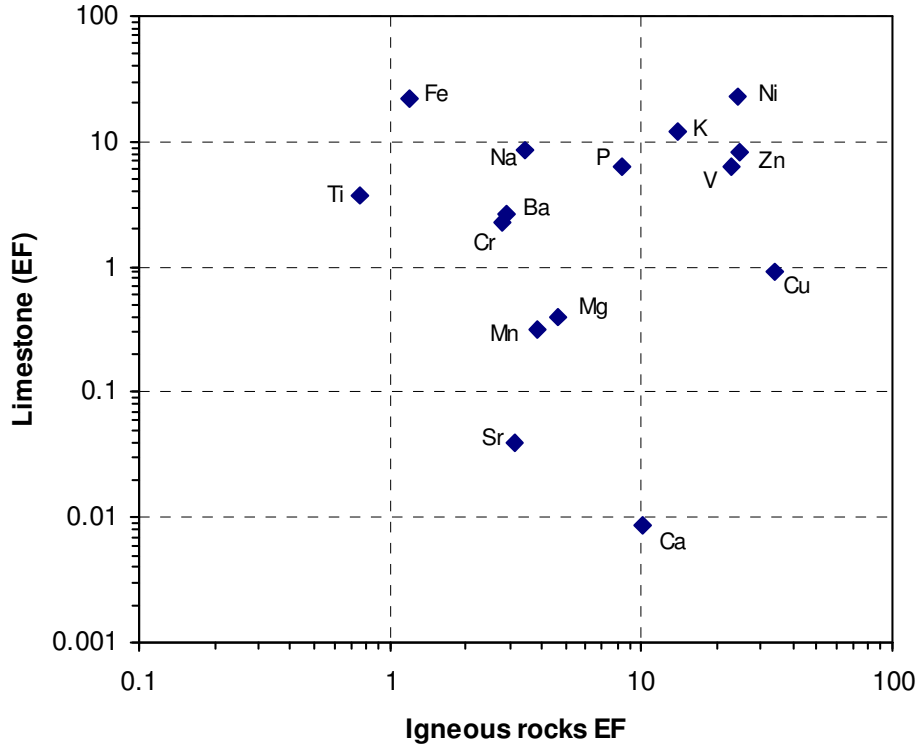

Fig. 7. Mean element enrichment factors in *T. recurvata* at Mezquital Valley.

ACPD
9, 5809–5852, 2009

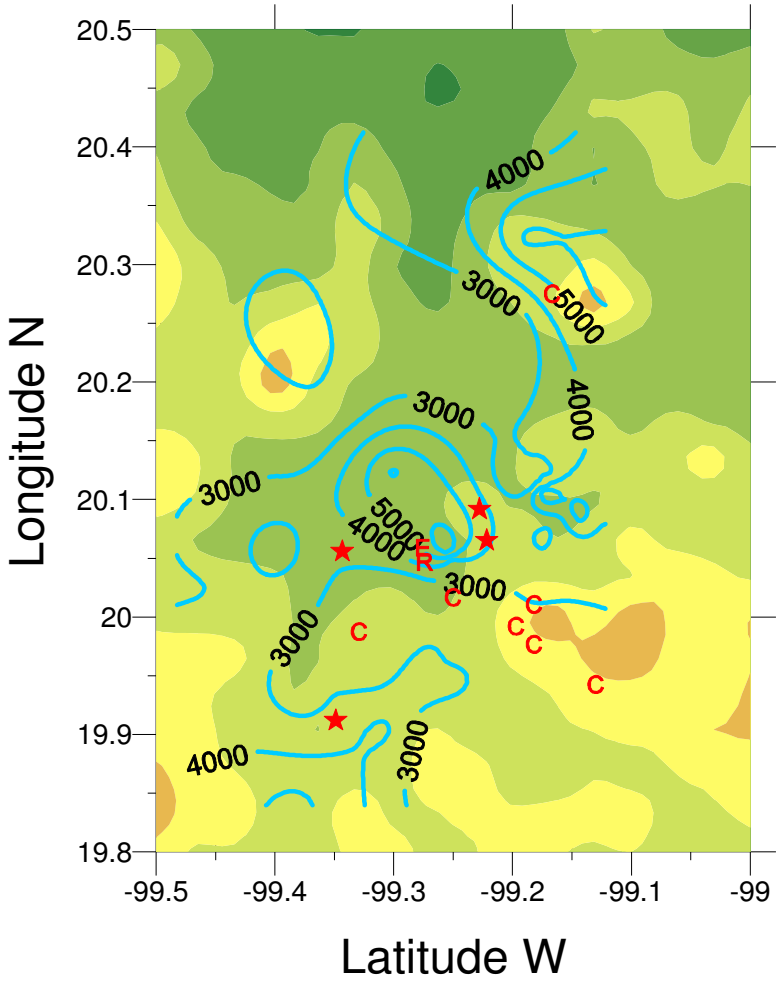

Fig. 8. Spatial distribution of Na in *T. recurvata* at Mezquital Valley.

ACPD
9, 5809–5852, 2009

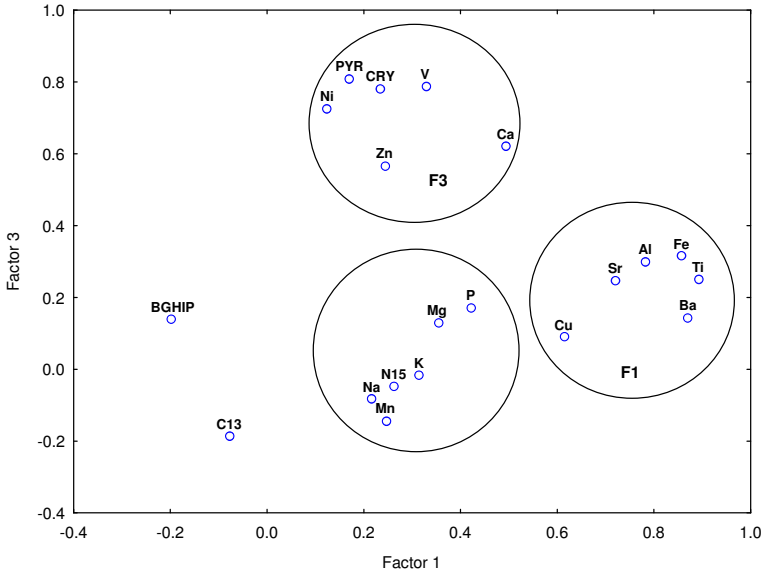

Fig. 9. Factor 3 vs. factor 1 plot. F1 includes elements from mainly crustal origin; F3, elements and PAH from petroleum fuel combustion and cement production (Ca). The third circle includes elements related to agriculture soil sources (F2, F4 and F5, not shown).

ACPD
9, 5809–5852, 2009